The land-sea coastal border: A quantitative definition by considering the wind and wave conditions in a wave-dominated, micro-tidal environment

Agustín Sánchez-Arcilla[1], Jue Lin-Ye[1], Manuel García-León[1], Vicente Gràcia[1], and Elena Pallarès[1,2]

[1]Laboratory of Maritime Engineering, Barcelona Tech, D1 Campus Nord, Jordi Girona 1-3, 08034, Barcelona, Spain
[2]EUSS - Escola Universitaria Salesiana de Sarria, Sant Joan Bosco 74, 08017, Barcelona, Spain

Correspondence: A. Sánchez-Arcilla (agustin.arcilla@upc.edu)

Abstract. A quantitative definition for the land-sea (coastal) transitional area is here proposed for wave-driven areas, based on variability and isotropy of met-ocean processes. Wind velocity and significant wave height fields are examined for geo-statistical anisotropy along four ~~perpendicular~~ cross-shore transects on the Catalan coast (northwestern Mediterranean) illustrating a case of significant changes along shelf. The variation of the geo-statistical anisotropy as a function of distance from the coast and water depth has been analyzed through heatmaps and scatter plots. The results show how the anisotropy of wind velocity and significant wave height decrease towards the offshore, suggesting an objective definition for the coastal fringe width. The more ~~robust~~ viable estimator turns out to be the distance at which the significant wave height anisotropy is equal to the 90^{th} ~~quantile of variance~~ percentile of variance of the anisotropies within a $100\mathrm{km}$ distance from the coast. Such a definition, when applied to the Spanish Mediterranean coast, determines a fringe of width of $2\text{-}4\mathrm{km}$. Regarding the probabilistic characterization, the inverse of wind velocity anisotropy can be fitted to a lognormal distribution function, while the significant wave height anisotropy can be fitted to a log-logistic distribution function. The joint probability structure of the two anisotropies can be best described by a Gaussian copula, where the dependence parameter denotes mild to moderate dependence between both anisotropies, reflecting a certain decoupling between wind velocity and significant wave height near the coast. This wind-wave dependence remains stronger in the central, bay-like part of the study area, where the wave field is being more actively generated by the overlaying wind. Such a pattern controls the spatial variation of the coastal fringe width.

1 Introduction

Land-sea border areas are narrow strips of water that display unique met-ocean dynamics due to a) non-linearity and sea bottom interactions (including bathymetric control) for the ocean ~~(?)~~ (?) and b) differential heat over land/sea and topographic control on winds (e.g. channeled winds and coastal jets) ~~(???)~~(??). This results in enhanced gradients that interact with very productive ecosystems and a large number of infrastructures and socio-economic uses related to tourism, fisheries/aquaculture or maritime transport ~~(???)~~(????). However, the limits of this land-sea transition remain fuzzy and even somewhat subjective, depending on the type of process or application considered and with technical, economic and legal implications.

There is, thus, a need for a systematic and objective definition of the coastal fringe that considers underlying processes and that has general applicability allowing for the time/space dynamics of this fringe. This type of approach has been explored in the literature, where for instance **?** reviewed a number of possibilities based on a dynamic balance of competing processes (i.e. drivers) such as inertial effects, geostrophic steering, sea bed friction or water column stratification. ~~**?** proposed a definition for the active beach profile, based on beach state and an environmental parameter function of the active hydrodynamics and the sediment fall velocity. The recent advent of high~~ Another suitable option is to focus on the consequences of such processes, such as the nearshore morphodynamic features (**?**) (i.e. deltas, sand spits, overwash fans, beach berms). Both complementary classifications requires spatial data that needs to be updated accordingly within timescales that may range from years (i.e. long-term erosion due to sea level rise) to days (i.e. storm-scale).

In the last decades, the advent of remote sensing has led to enviromental monitoring at spatio-temporal scales hard to achieve previously, with just in-situ measurements. Hence, such high spatial resolution and short revisit time ~~provided by the new Sentinel data (**??**)~~ offer an alternative source of information for such a coastal zone definition, although with some limitations since the data may start degrading at a few kilometres (order $10\mathrm{km}$) offshore from the coast ~~(**?**). Because of that it is necessary~~ (**???**). The land boundaries induce error in the satellite observations. Hence, it is useful to use high resolution numerical simulations supported by in-situ data so that land-sea boundary effects are properly captured for the subsequent coastal definition that will be based on the ~~inhomogeneity~~ heterogeneity introduced by the presence of the land boundary.

~~Anisotropy~~ The geo-statistical anisotropy (henceforth, anisotropy) in wind and wave fields (**?**) can be an useful indicator of spatial structure, affected by topo-bathymetric constraints that generate substantial gradients in met-ocean conditions ~~.~~ that are wave-driven. In this text, the term "anisotropy" refers only to the geo-statistical anisotropy, not the geo-physical one. A wind or wave field that has a high anisotropy can present a predominant wind or wave direction, respectively. It is well known that the geo-statistical anisotropy can be a measure to define directional variation e.g. for mineral configuration in rocks (**?**), for propagation velocity in heterogeneous media (**?**) or for seismic waves (**?**). Similarly, topographic induced geo-statistical anisotropy affects coastal wind patterns that force wave and current fields (**?**).

The aim of this paper is to analyse ~~coastal anisotropy and from that~~the geo-statistical anisotropy of nearshore wind and waves, in wave-driven coasts. From that, what follows is to propose a new quantitative and objective definition for the land-sea border that benefits from these high-resolution (spatial and temporal) ~~wind and wave fields (**?**)~~ fields and from the underlying process-based knowledge. This definition can be useful to determine a set of criteria for numerical purposes (e.g. nesting coastal domains) but also for more practically oriented applications (e.g. offshore limit for outfall dispersion). The analysis is based on a set of high-resolution wind and wave fields in the latter case using a well-tested code such as SWAN ~~(**???**)~~(**????**). The numerical results, pertaining to a micro-tidal environment to avoid any distortion of spatial patterns by tides, will be subject to inexpensive statistical methods to characterize spatial structures. Following this approach, the paper is structured as follows. Section 2 introduces the theoretical background. Section 3 describes the study area, while the methodology is presented in Section 4. Section 5 lists the main results, which are discussed in Section 6, followed by some conclusions in Section 7.

2 Theoretical background

~~Anisotropic data fields are easily convertible to isotropic ones through rotation and rescaling (?). Being u and v the axes of the two principal directions~~ Given a spatio-temporal field $X(s,t)$, where s stands for a 2-D vector (zonal and meridional components) and t is the time, it is assumed that the iso-level contours of the correlation functions are invariant, i.e. ellipses in two dimensions. The main axis of these ellipses are termed u and v, respectively (see Fig. 1)~~, being θ ($\theta \in [0, 2\pi)$) the rotation in respect the principal coordinate system and~~. The metric of the geometric anisotropy, then, becomes their ratio $R = \frac{u}{v}$ ($R \in [0, \infty)$) ~~the ratio between the principal axes of anisotropy, the new axes of the two principal directions can be obtained as:~~

$$u^* = u\cos\theta + v\sin\theta$$

$$v^* = (-u\sin\theta + v\cos\theta)\, R.$$

~~From this definition, it is aparent that R can serve to quantify the anisotropy of a data field~~(??). An R value close to unity means that u and v are isotropic, i.e. homogeneous across the different directional sectors. As R increases, the difference between the main axis increase, showing higher anisotropy at certain directional sectors.

Considering the ratio R as a ~~variable for any 2D field~~1-D random variable, it can be fit to a probability distribution function. Such fitting depends on theoretical and practical considerations. The preferred shape is determined by looking at statistical characteristics such as mean, variance, skewness and kurtosis, or by examining the similarity between quantiles (dataset versus theoretical probability distribution) using a Quantile-Quantile plot. The more direct candidates to fit variable R are a) the log-normal function, where the probability distribution of its log-transform is Gaussian (**?**) and b) the log-logistic function, with a logistic probability distribution for the log-transformed variable. A logistic distribution has a probability density function of the form:

$$f(x) = \frac{1}{s}\exp\left((x-m)/s\right)\left(1+\exp\left((x-m)/s\right)\right)^{-2}, \tag{1}$$

where m is its location parameter and s is its scale parameter.

Sklar's theorem (**?**), expresses the multivariate joint probability structure of two variables x and y as the product of their cumulative probability distributions ~~$F(x) = u$ and $G(x) = v$ (u and v here are not yet related to any definition of anisotropy)~~$F(x)$ and $G(y)$, and a 2-D copula. The interval of variation of ~~u, v~~ $F(x)$, $G(y)$ is $[0,1]$ and a 2-D Gaussian copula has the form:

$$C_\rho\left(uF\left(x\right), vG\left(y\right)\right) = \int_{-\infty}^{\Phi^{-1}(u)\Phi^{-1}(F(x))} \int_{-\infty}^{\Phi^{-1}(v)\Phi^{-1}(G(y))} \frac{1}{2\pi\sqrt{1-\rho_{12}^2}} \exp\left\{-\frac{s^2 - 2\rho_{12}st + t^2}{2\left(1-\rho_{12}^2\right)}\right\} \mathrm{d}s\mathrm{d}t. \tag{2}$$

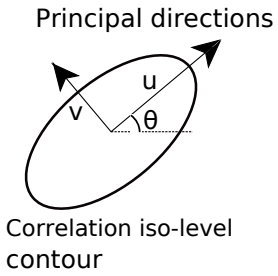

Figure 1. ~~Transformation between anisotropic and isotropic~~ Representation of a generic ellipse that represents the geo-statistical geometric anisotropy of a wind or wave fields. Supposing u and v are the two principal directions of anisotropy, ~~any given anisotropic correlation iso-level contour can be converted into an isotropic one using~~ the anisotropy ratio is $R = \frac{u}{v} > 1$~~and a certain~~ . θ is the rotation angle ~~θ. The new~~ of the field~~has a ratio $R^* = \frac{u^*}{v^*} = 1$~~.

where the correlation parameter $-1 < \rho_{12} < 1$ is used as the dependence parameter and Φ is the univariate standard normal distribution function (**?**). $\rho_{12} = 0$ means total independence between the variables, whereas $|\rho_{12}| = 1$ means total dependence. Whenever a joint probability structure has the form of a Gaussian copula, this structure can be applied without excessive computational cost (**??**), compared, for instance, to an Archimedean copula approach (**???**).

3 Study area

The selected pilot site for application is a wave-driven and micro-tidal environment such as the western Mediterranean Sea (Fig. 2), where enough validated met-ocean simulations exist and where the spatial wind/wave structure will not be distorted by tidal forcing. Current fields, slower to respond to the overlying meteorological driving, have not been considered in this initial analysis. The focus is on the Spanish north-eastern Mediterranean coast, where we have in-situ ~~data available and Sentinel images~~ and altimeter data for support. Moreover, the continental shelf varies in from 10km to more than 100km in an alongshore distance of less than 500km. The wind fields are affected (most frequent wind direction is from land, corresponding approximately to the north-west) by the presence of a mountain chain roughly parallel to the coastline and featuring several openings corresponding to river valleys. The geometrical anisotropy analysis has been performed at four ~~characteristic transects, in terms of~~ transects, characteristic of its common topo-bathymetric features. They correspond (Fig. 2) to the following locations (from south-west to north-east): Ebre (40.7°N, 0.87°E), Tarragona (41.12°N, 1.25°E), Mataro (41.53°N, 2.45°E) and Begur (42.28°N, 3.02°E).

The north-western Mediterranean presents a particularly intense wind forcing~~(??)~~, which is shaped by local orography ~~(?)~~ (??). The Pyrenees mountain chain across the strip of land connecting the Iberian Peninsula to the European Continent forces a strong northern wind flux following the French-Spanish Mediterranean coast (**???**). This same wind pattern is channelled by the river valleys resulting in a north-western orientation for winds blowing from land to sea further down along the coast (**?**), for latitudes southward of $41°N$. The most frequently observed patterns are, thus, from North in the coastal sector closer

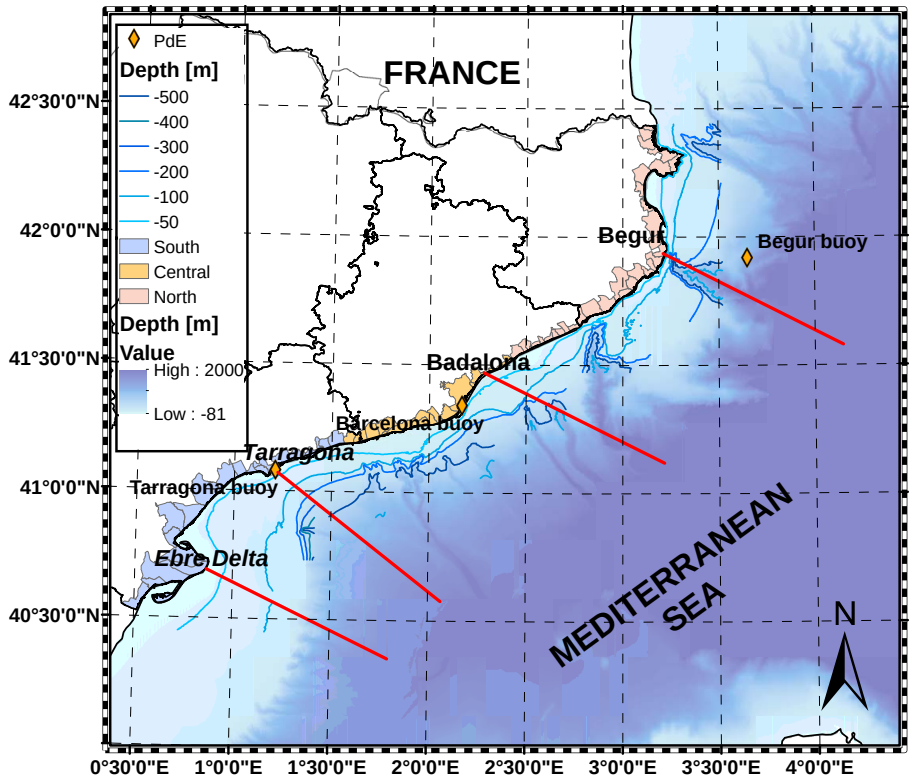

Figure 2. Study area, showing the gradients in topo-bathymetry that exert a strong control over the resulting met-ocean conditions. There are depicted the four transects (red lines) used to estimate the limit of the coastal fringe, located in (from South to North): a) Ebre Delta, b) Tarragona, c) Badalona and d) Begur. It also shows the Puertos del Estado (PdE) buoys and the division of the Catalan Coast into the northern, central and southern sections (different colours in the land part).

to the Pyrinees barrier and from the northwest further south, conditioned by the river valleys and gaps in the coastal parallel mountains ~~(???)~~(??). The second most frequent pattern corresponds to western winds, associated to atmospheric depressions in northern Europe ~~(??)~~(???). Easterly winds are frequent during the summer, triggered by an intense high-pressure area over the British Islands.

The most common wave fields in the north-western Mediterranean Sea correspond to wind-sea ~~(??)~~ (??) forced by the easterly winds ~~(?)~~ and the northerly and north-westerly winds mentioned above. Because of the semi-enclosed character of the basin, the waves are fetch-limited~~(?)~~, with maximum trajectory lengths around $600\mathrm{km}$, one-sixth of the average distance that a wave train travels across the Atlantic (**?**). The average wave-climate in the north-western Mediterranean Sea presents a mean significant wave height (H_s) of $0.78\mathrm{m}$ at the southern part of the Catalan coast, near the Ebre delta and slightly lower values (around $0.72\mathrm{m}$) further north and close to the French border. The spatial distribution for wave storms presents an opposite ~~behaviour~~trend, with maximum H_s between $5.48\mathrm{m}$ in the southern sector and $5.85\mathrm{m}$ at the northern coastal stretch ~~(??)~~(?) . Future projections **?** indicate, for the interval 2071-2100 and A1B scenario (**?**) a variation of the significant wave height

around $\pm 10\%$, whereas the same variable for a 50year return-period exhibits rates of change around $\pm 20\%$. Additionally, the variability in large-scale indices (i.e. NAO, EA or Scandinavian Oscillation) may drive significant changes in wave storm components (?).

4 Methods

The approach suggested for ~~an objective assessment of anisotropy (leading to an automated definition of coastal boundaries) is schematized~~ assessing the geo-statistical anisotropy of wind and wave fields is schematized in (Fig. 3). It requires high-resolution met-ocean fields to determine how the covariance of ~~anisotropy evolves~~ the geo-statistical anisotropies of wind and wave fields evolve with distance to the land-sea border. The starting point are wind and associated wave fields, as the ~~most promising~~ suggested candidates for reflecting the ~~inhomogeneity~~ heterogeneity induced by coastal topo-bathymetry. Although other definitions of the coastal boundary can be based on river plumes or bio-geochemical processes, it has been intended to focus on a more hydro-dynamical expression of such boundary for wave-driven coasts. It is intended to show that, as one approaches the coast, the wind and the wave fields should present a greater geo-statistical anisotropy, that is, they should display predominant wind and wave directions. Furthermore, there should be a geo-statistical boundary to the value of this anisotropy that could help define a coastal boundary.

The wind fields have been provided by the UK-Met Office, from their Unified Model (?) for weather and climate applications. This code solves the compressible, non-hydrostatic equations of motion with semi-Lagrangian advection and semi-implicit time stepping, including suitable parameterizations for sub-grid scale processes such as convection, boundary layer turbulence, radiation, cloud microphysics and orographic drag (?). There are two atmospheric prognostics: the dry one (three-dimensional wind components, potential temperature, Exner pressure and density) and the moist one (specific humidity and prognostic cloud fields (?). Both long and short radiations (from the sun and the Earth itself) are included, whereas the effect of aerosols reflecting them is taken into consideration. These wind data has been validated in previous works, such as in ?.

The computational domain ~~covers the entire~~ of the wind field spans the whole Mediterranean Sea using a regular grid with spacing of ~~$\Delta\phi = 2.5°$ for latitude, of $\Delta\lambda = 3.75°$ for longitude~~ 17km and a time step of 1h. The ~~associated~~ wave fields have been calculated with the SWAN code, covering the same geographical domain and with equal time step of 1h. SWAN is a spectral wave model based on the wave action balance equation ~~(?) and including wave-wave~~ (??) that includes non-linear interactions at various depths and ~~whitecapping~~dissipation processes (i.e. whitecapping, bottom friction, wave breaking). It applies a fully implicit numerical scheme for propagation in geographical and spectral spaces that is unconditionally stable.

SWAN employs an unstructured grid with spatial resolutions of 600m-40km, ~~higher~~ denser near the land-sea boundary. Mesh sizes are ~~determined objectively based on~~ proportional to bathymetry gradients and distance to the coastline~~(?)~~, following the same criteria than in (?). Such a non-structured grid approach avoids nesting and internal boundary conditions, while maintaining a good spatial resolution to capture bottom and coastline irregularity (submarine canyons and capes or prodeltas that are found in the Catalan continental shelf). Furthermore, unstructured meshes are well suited to tackle non-linear effects ~~(???)~~ (???). The resulting wave fields have been validated with two directional wave buoys at the northern ~~and southern~~ (Begur,

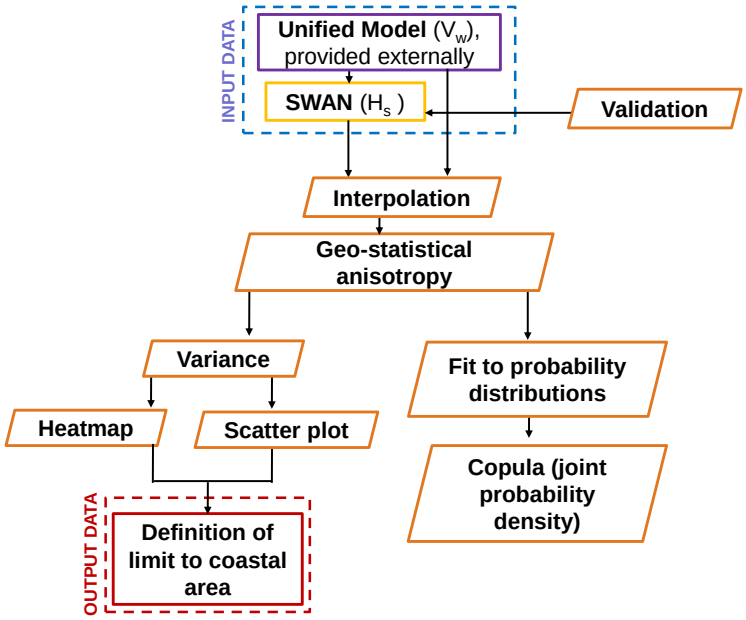

Figure 3. Flow-chart summarizing the methodology used in this paper. The dashed blue rectangle represents the input data, the red dashed rectangle indicates the output data. The wind velocity is obtained from an external source, and it was validated in **?**. The rest of the ~~green dashed rectangle shows the present~~ steps have been carried out for this analysis. Rectangles indicate data generation (input/output) and rhombuses, the subsequent analyses of the proposed methodology.

deployed at 1200 m) and southern (Tarragona coastal buoy, deployed at 15 m) ends of the domain, managed by Puertos del Estado (Fig 2). Altimeter data from three satellites (Cryosat,Jason-2 and Jason-3) are also used as a complementary observational source. The simulation period ranges from October 2016 to March 2017.

~~The independent variables used for analysing anisotropy are distance to the coast (x) and water depth (h) . The anisotropy has been computed for the~~ Once obtained the wave outputs, the empirical semi-variograms for the significant wave height and the wind velocity at 10m ~~over the mean sea-level (R_{V_w}) and for the significant~~ are estimated. In order to have enough data, the spatial radius of influence is assumed to be 5km, plus time blocks of 24 hours. From these semi-variograms, the anisotropy for the wave height (R_{H_s}) ~~.~~ and the wind velocity (R_{V_w}) is estimated along the four transects in Fig 2.

Distance to the coast (x) and water depth (h) are selected as independent variables for analysing the anisotropy spatial patterns. R_{V_w} and R_{H_s} are taken to represent the behaviour of met-ocean conditions under the effect of the land-sea boundary (in this initial analysis height/depth gradients in topo-bathymetry). ~~They have been calculated~~ Hence, R_{V_w} and R_{H_s} have been interpolated (1km spacing) along a 100km transect perpendicular to the coast (see Fig. 2), considering periods of 24h, long enough for the waves to respond to the acting wind forcing.

The geo-statistical Anisotropy needs to be computed on a regular grid and therefore, both wind velocity (V_w) and significant wave height (H_s) have been interpolated on a rectangular mesh~~.~~, first on a grid of 1km then to a finer mesh of 10m.

The interpolation method used in this case is the inverse distance weighted (IDW) interpolation, that estimates the value at an interpolated location (x) as the weighted average of neighbouring points with weights $w(x)$ given by

$$w(x) = \frac{1}{d(x, x_i)^p}. \tag{3}$$

Here, x_i is a neighbour point, d is the Euclidean distance and p is the inverse distance weighting power. The IDW power chosen is 1 for R_{V_w} and 3 for R_{H_s} and h, based on a sensitivity analysis for this area and consistent with the physical relation between wind velocity and generated wave height.

~~R (R_{V_w} or R_{H_s}) values are calculated for clusters of V_w or H_s within a circular sub-domain with radius of 5km.~~ Heatmaps are used to represent the spatial distribution of the geo-statistical anisotropy, showing how the density of R behaves as a function of distance to the coast and time (see Figs. 6 and 7). These maps are scatter plots that act as a 2D-histogram, in which two variables (in this case, R and distance to the coast) are grouped in pre-defined intervals. The elements selected to aggregate samples for the heatmap are hexagons with side 5km and a scale for anisotropy of 20 units for both R_{V_w} and R_{H_s}. Both R and its variance are calculated on a discrete number of distances to the coastline, assuming that the width of the fringe affected by boundary effects is below 100km for this coastal sector (**?**). From here, ~~it follows naturally to propose a~~ as is with significant wave height to determine the presence of wave-storms (**??**), the proposed coastal zone limit ~~as~~ is the cutting point where the variance of R is equal to the 90^{th} ~~quantile~~ percentile of the total R variance spanning a fringe between 0 and 100km:

$$l = 90^{th}\ quantile percentile\ of\ \mathrm{var}\left(R_{H_s}\left(0\mathrm{km} \leq x \leq 100\mathrm{km}\right)\right) \tag{4}$$

This cutting point has shown, as expected, larger stability for the wave field than for the forcing wind patterns. The variation of R_{H_s} with coastal distance x (Fig. 7) indicates for reference the 20km distance where satellite data offer enough robustness ~~(?)~~ (**???**). The plot also displays depth against x~~, after interpolation into a regular mesh (first on a grid of 1km, then to a finer mesh of 10m)~~. The obtained R_{V_w} and R_{H_s} values have been fit to a probability distribution, selecting empirically the lognormal function for the inverse of R_{V_w} and the log-logistic function for R_{H_s}. ~~The joint probability has been next~~ Once estimated the marginal distributions, the dependence structure of the joint probability is adjusted to a Gaussian copula ~~to capture the partial dependence structure.~~ (see Sec. 2).

5 Results

The ~~SWAN model simulations~~ modelled wave heights (H_s) have been validated with ~~registered significant wave height (H_s)~~buoys from the Puertos del Estado monitoring network and available altimeter data (Jason-2, Cryosat and Jason-3). Two locations have been selected, located at the southern (Tarragona~~location~~) and northern (Begur~~location~~) coastal sectors (Figs.

Table 1. Statistics of the agreement between numerical significant wave height fields (SWAN model) and observations in terms of root mean square error (R.M.S.E.), bias and scatter index (S.I.) for the control points at the southern and northern coastal sectors.

Buoy	R.M.S.E. [m]	bias [m]	S.I. [%]
Tarragona coastal buoy	0.248	−0.132	0.502
Begur	0.393	−0.087	0.249

4 and 5). The H_s buoy data show ~~substantial coincidence~~ good agreement with the simulated H_s, quantified in table 1 and in Figs. 4 and 5.

In general, the wave model performs better at deep waters than in coastal waters. The standard deviation is higher in the model than in the observations. At Begur, the bias and the Scatter Index are lower, whereas the RMSE is higher (Tab. 1). At the same buoy, the correlation coefficient is near 95% and the difference between standard deviations is lower (0.2m vs. 0.4m). Note that the Northern part of the Catalan coast is more energetic than the Southern one (see Fig. 5). For instance, in Begur the storm peaks can reach about 7m, whereas at Tarragona the highest recordings are 3.5m.

The altimeter collocated has a positive bias in the coastal zone, and the opposite (i.e. negative bias) happens at deep waters. Nevertheless, there exists qualitative consistency between the in-situ and remote-sensing sources. Additionally, SWAN has been able to capture the regime switching and the proper timing of the storms, despite it tends to underestimate the magnitude of the storm peaks.

R_{V_w} and R_{H_s} have been analysed with heatmaps (Figs. 6 and 7) and scatterplots (Figs. 8 and 9). R_{V_w} presents values that span ~~the interval~~ from 1 to 250 and display a dependence on coastal distance (Fig. 6), featuring a combination of anisotropy close to the land boundary (0 to 20km) and then more isotropic behaviour towards the offshore (up to 100km), although with a rich variability. The wind fields present, in summary, a decreasing variance from 0 to 100km with a pronounced slope from 0 to about 40km (southern sector) or even further offshore (northern sector) and then an almost asymptotical trend. R_{H_s} behaves similarly to R_{V_w}, but with a turning point at about 40km in all transects (Figs. 8 and 9) and, thus, a higher level of consistency. From December to January, there are some winds and waves registered within 20km of the coast that present higher R_{V_w} and R_{H_s}, however, they are so few that the variances of R_{V_w} and R_{H_s} in this area do not differ from warmer seasons. Therefore, there is not a clear seasonality to the R_{V_w} or the R_{H_s}. The ~~limit l~~coastal zone limit l, corresponding to the 90^{th} ~~quantile~~ percentile of the total variance (fringe between 0 and 100km), is calculated from equation 4 (Figs. 8 and 9) and ~~presents small differences~~ is 3km. It is consistent with time interval (month of study) and location (sector)~~, below the 1km limit~~.

In order to find a copula structure, marginal probability distributions for the two anisotropies are needed. Skewness and kurtosis from the analysed data show that the inverse anisotropy of V_w follows a log-normal distribution, while the anisotropy of H_s follows a log-logit distribution. Quantile-quantile plots have been used to assess the fit of each probability function (not shown here) to its target dataset, verifying that the selected samples can be adjusted to the corresponding probability distributions. The joint probability structure of the two anisotropies does not present any marked dependence for the ~~largest~~

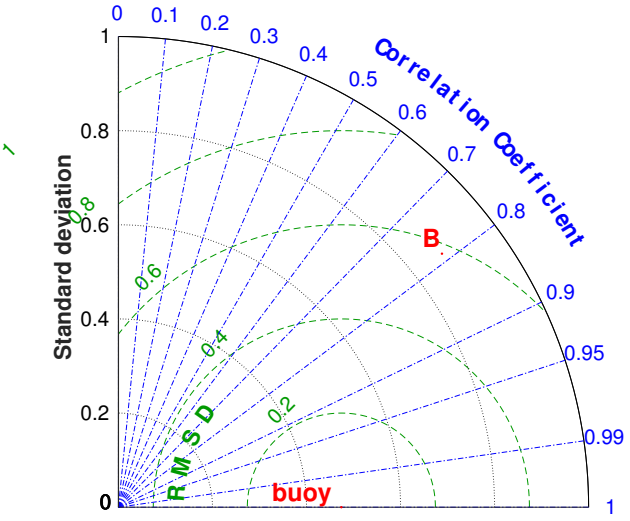

[a]

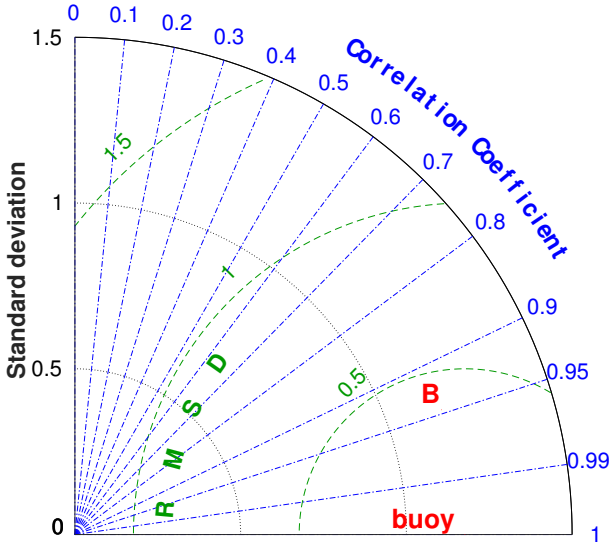

[b]

Figure 4. Taylor diagram for the significant wave height (H_s) showing correlation, standard deviation and root mean square error (R.M.S.E.) between numerical and observed data for a) south sector (Tarragona location) and b) north sector (Begur location)~~, for the~~. The time period ranges from November of 2016 to March of 2017.

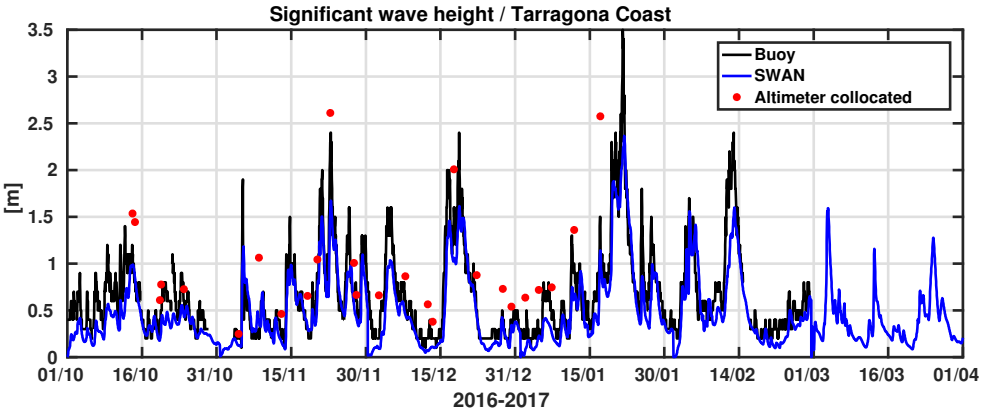

[a]

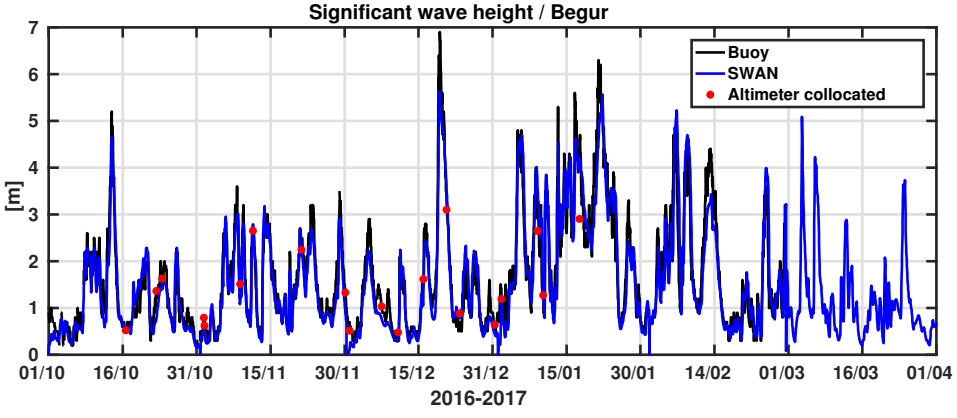

[b]

Figure 5. Comparison of numerically simulated significant wave height (SWAN model) with observations, for a) south sector (Tarragona location) and b) north sector (Begur location), for the period ~~November~~ October of 2016 to March of 2017. The red dots are altimeter data from the available altimeter data (Jason-2, Jason-3 and Cryosat).

~~(tail) values~~upper-tail percentiles, suggesting the use of a Gaussian copula, whose dependence parameter ρ is shown in Fig. 10. The so obtained dependence ranges from total independence (0) to a mild ($|\rho_{12}| = 0.1$) dependence between R_{V_w} and R_{H_s}.

6 Discussion

The calculated anisotropies should be as robust as the starting wave or wind fields that are employed in the analysis. Because of that, the SWAN code has been calibrated with local atmospheric and hydrodynamic conditions (?). Special emphasis has been put on using high quality wind fields, both for the direct assessment linked to meteo fields and for the indirect effect they exert on the behaviour of the forced hydrodynamics. The results show, as expected, a higher level of robustness for the wave-based geo-statistical anisotropy, where the calculations used an unstructured grid and a locally adjusted whitecapping term calibration

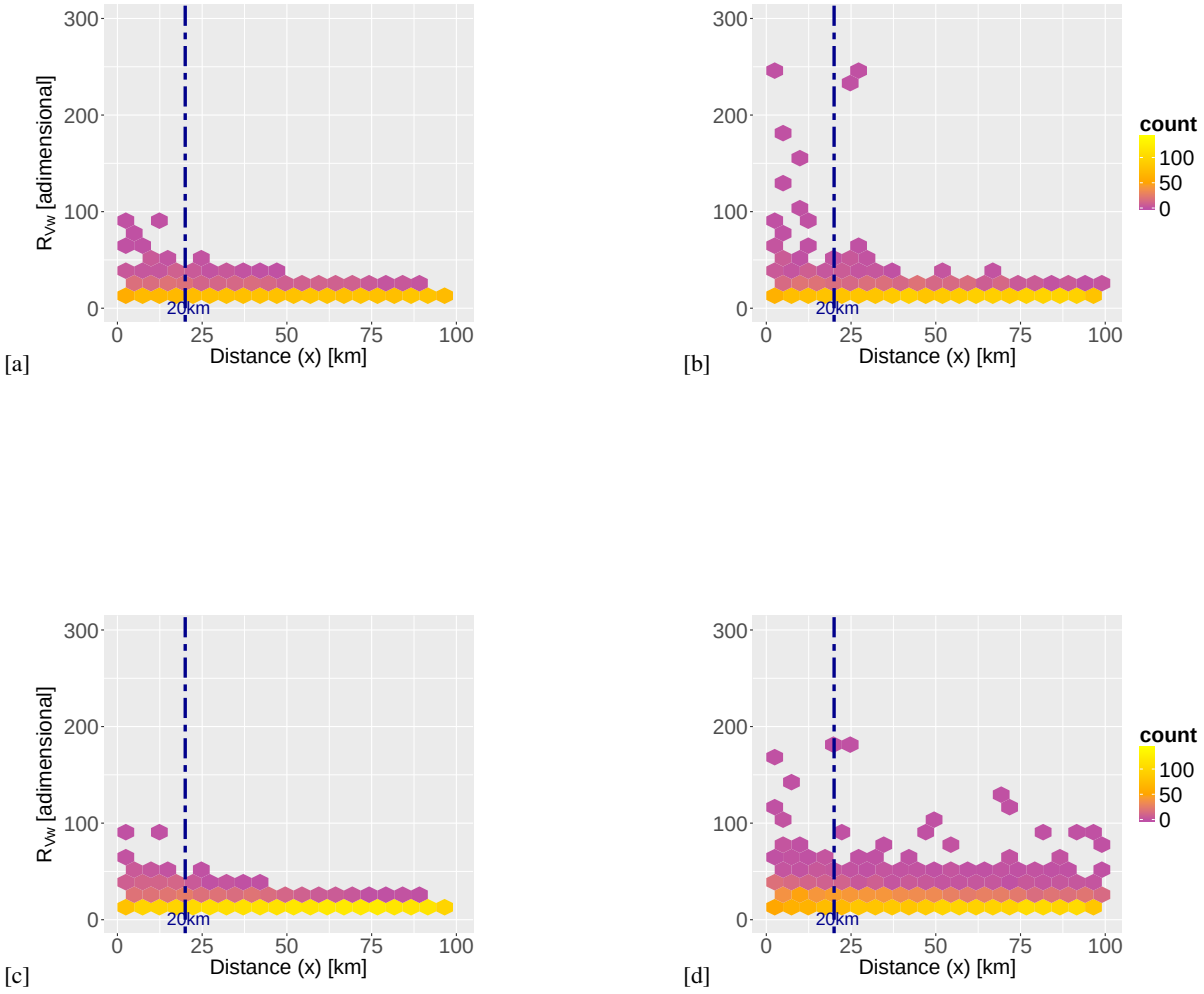

Figure 6. Heatmap of the geo-statistical anisotropy ratio of the wind velocity (R_{V_w}) against distance to the coast for a) south control transect (near the Ebre delta), b) central-south transect (near Tarragona harbour), c) central-north transect (near Mataro harbour) and d) north control transect (near Begur cape). The elements selected to aggregate samples for the heatmap are hexagons with side 5km and a scale for anisotropy of 20 units. The counts are the number of elements within a hexagon. A limit of rough order of magnitude for the direct applicability of remote-sensing data (20km) is also shown (blue dashed line). All plots correspond to February 2017.

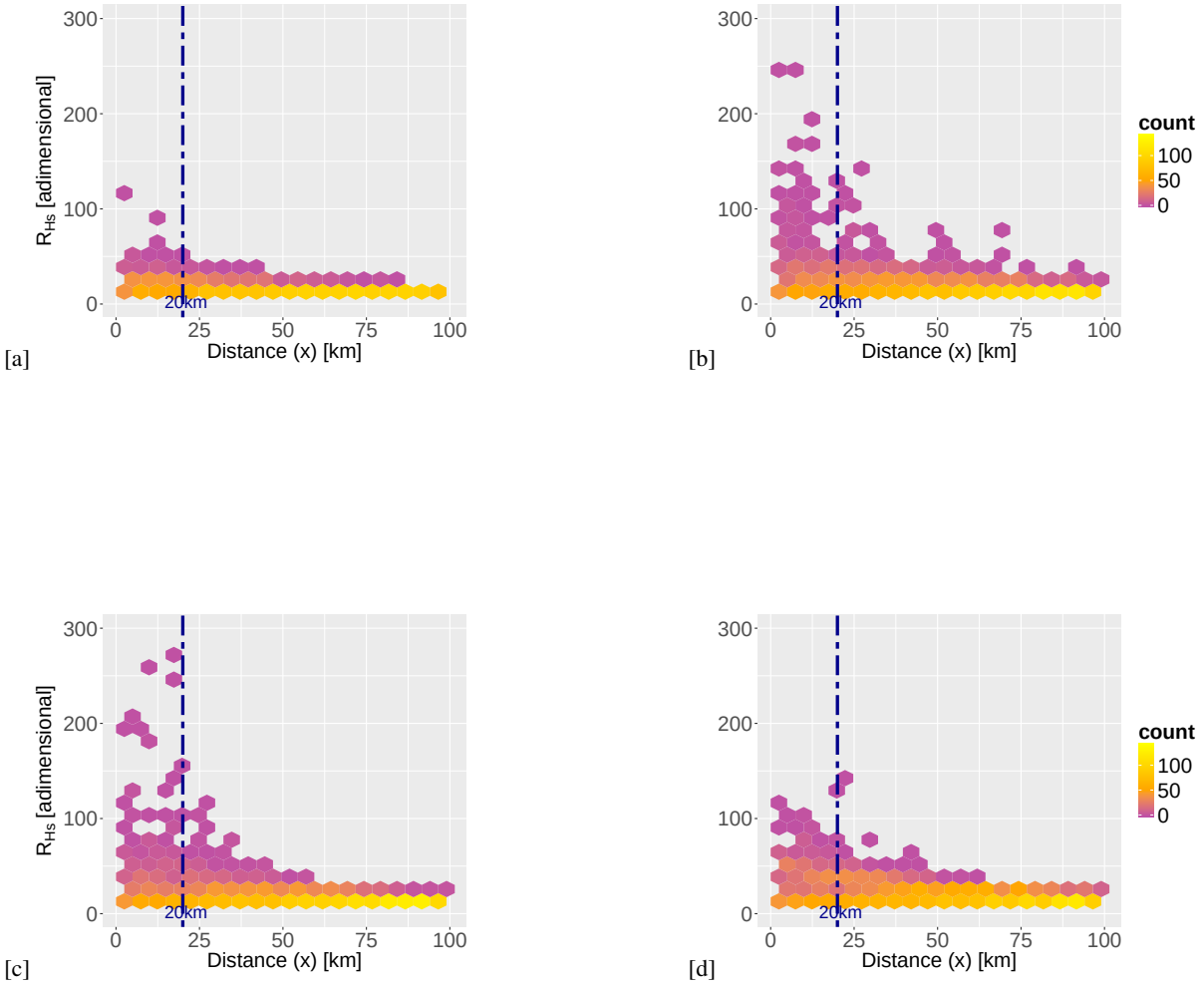

Figure 7. Heatmap of the geo-statistical anisotropy ratio of significant wave height (R_{H_s}) against distance to the coast for a) south control transect (near the Ebre delta), b) central-south transect (near Tarragona harbour), c) central-north transect (near Mataro harbour) and d) north control transect (near Begur cape). The elements selected to aggregate samples for the heatmap are hexagons with side 5km and a scale for anisotropy of 20 units. The counts are the number of elements within a hexagon. A limit of rough order of magnitude for the direct applicability of remote-sensing data (20km) is also shown (blue dashed line). All plots correspond to February 2017.

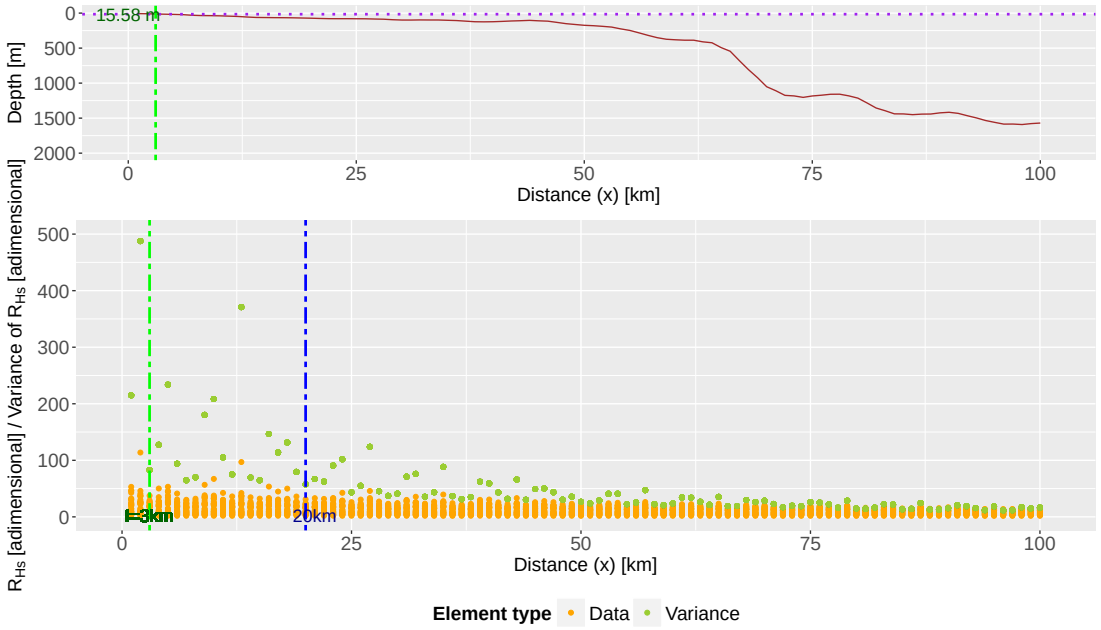

[a]

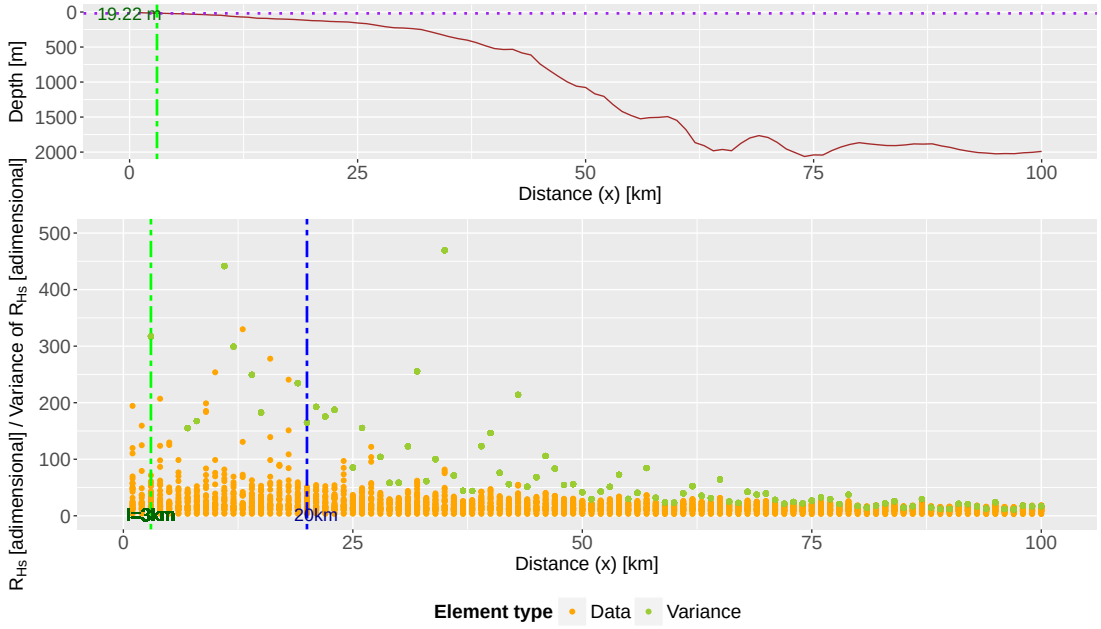

[b]

Figure 8. Relation for winter conditions (February 2017) between distance to the coast x, depth (upper plot) and anisotropy ratio of significant wave height (R_{H_s}), from shore to 100km offshore. Locations are a) south control transect (near the Ebre delta) and b) central-north transect (near Mataro harbour). The distance of 20km which has been suggested as a rough order of magnitude limit for direct applicability of ~~Sentinel~~ remote-sensing data is also shown (blue dashed line) together with the variance of R_{H_s} across the transect. From here, the coastal zone anisotropy-based boundary has been calculated and is also depicted. A green dash-dot line delimits its horizontal distance from the coast, whereas a purple dotted line denotes its elevation.

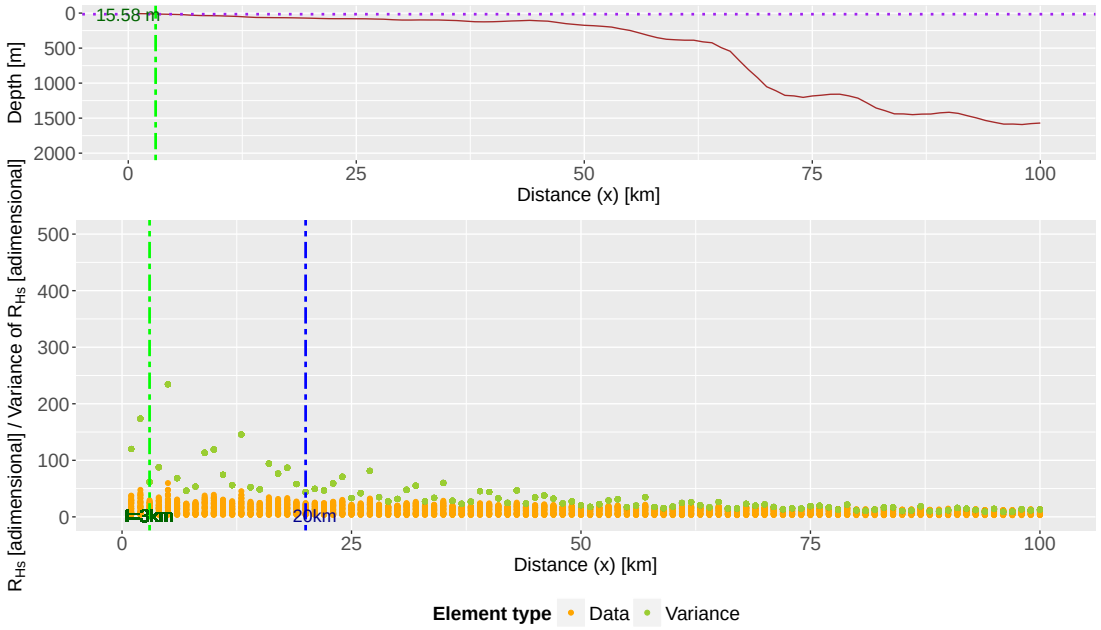

[a]

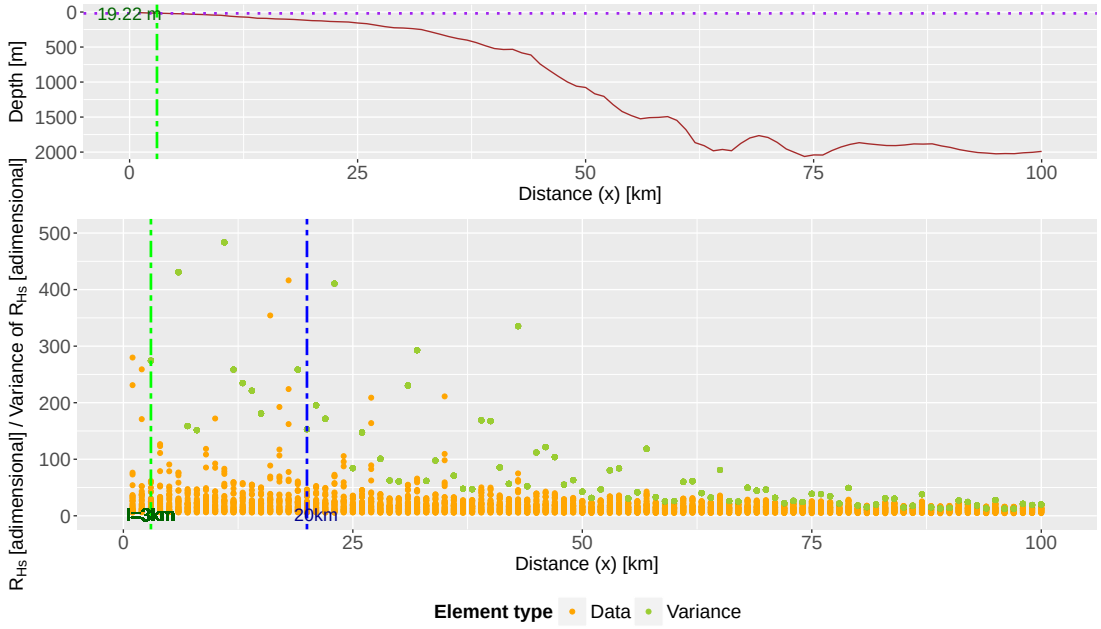

[b]

Figure 9. Relation for ~~end of summer~~ autumn conditions (November 2016) between distance to the coast x, depth (upper plot) and geo-statistical anisotropy ratio of significant wave height (R_{H_s}), from shore to 100km offshore. Locations are a) south control transect (near the Ebre delta) and b) central-north transect (near Mataro harbour). The distance of 20km which has been suggested as a rough order of magnitude limit for direct applicability of ~~Sentinel~~ remote-sensing data is also shown (blue dashed line) together with the variance of R_{H_s} across the transect. From here, the coastal zone anisotropy-based boundary has been calculated and is also depicted. A green dash-dot line delimits its horizontal distance from the coast, whereas a purple dotted line denotes its elevation.

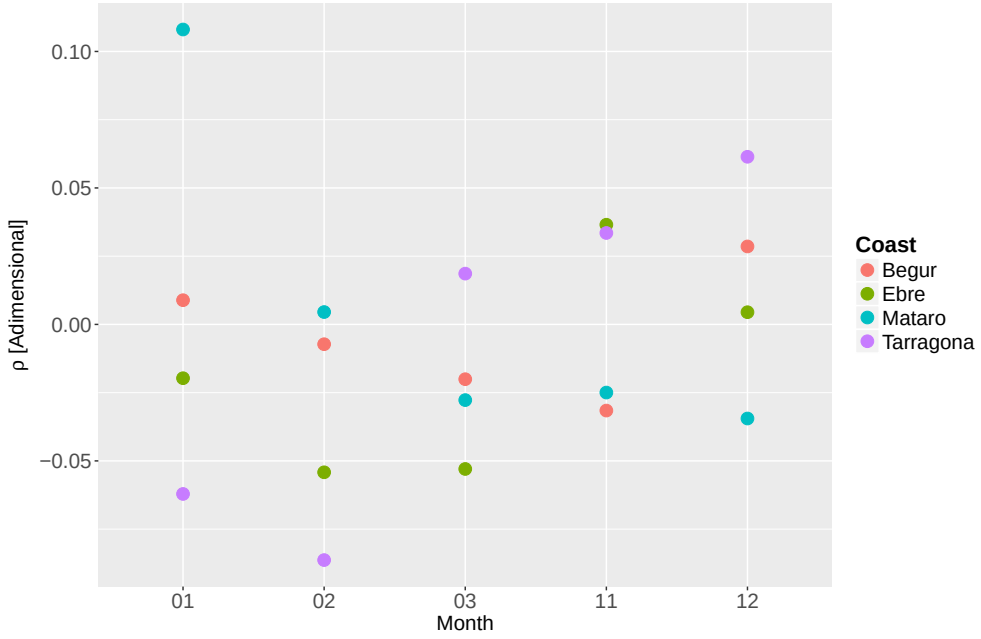

Figure 10. Copula parameters ρ of the proposed Gaussian copulas for all considered profiles: a) south control transect (near the Ebre delta), b) central-south transect (near Tarragona harbour), c) central-north transect (near Mataro harbour) and d) north control transect (near Begur cape). The plot shows the variation with time (horizontal axis) ~~for five different months within~~ between November of 2016 and March of 2017. The parameters are placed in a ~~year cycle~~manner that they start from January.

~~(??)~~(?). The cell size has been determined as a function of depth and distance to the coast~~(?)~~, consistently with the transect analyses performed in the paper. The application of an unstructured grid allows reducing computational costs (by about 50%) and the troublesome imposition of internal boundaries~~, which facilitates multiple simulations to perform a statistically stable analysis of anisotropy.~~.

This leads to an efficient determination of the coastal water boundary that ~~automatically incorporates some of the processes (e.g. turbulence levels in the water column due to wave action) and~~ contains some of its common geometric settings (e.g. bathymetric gradients affecting wave fields). Other processes, such as for instance the continental discharge, are of course not captured by the present analysis and would require a similar approach based on the resulting circulation fields, which would certainly capture the regions of fresh-water influence ~~.~~ and wave-current interactions (?). However, the performance of the wave model has shown commonalities with previous studies. For instance, the good performance of spectral models at the Begur buoy can be found in multi-model comparisons (see ?); and so the consistent underestimation under storm peaks (?).

The anisotropy-based approach will lead to different results depending on met-ocean conditions (wave conditions in our case), requiring a reliable simulation of both average and extreme patterns, as shown by the validation process (see e.g. Figs. 4 and 5). The transfer of energy from the coastal to the offshore domain and vice-versa ~~(?)~~ may condition the results of the analysis for areas near the transition, which is where the boundary will be likely located. This suggests a combined approach,

using numerical fields and satellite data supplemented by along-track in situ observations, all suitably interpolated in space and time to provide a picture that is as consistent as possible.

The values of V_w, H_s and h obtained through the IDW interpolation, using an IDW weighting from 1 to 3, are similar and reasonable. For marine variables the weight of 3 has been selected, to account for the influence of the closest neighbours based on the water inertia (which is 3 orders of magnitude larger than for air). The proposed IDW power for V_w is smaller because gas is more turbulent than water and thus should have a smaller spatial dependence. The obtained pattern for R_{V_w} is consistent for the four selected transects in the study area, showing a mostly isotropic behaviour for coastal distances from 0 to 100km. Higher values of R_{V_w} at distances from the coast below $20\mathrm{km}$ (see Fig. 6) indicate a clear directional spread of winds within the coastal fringe, linked to orographic control such as channelling by local mountains and river valleys.

Despite that the mainly shown results are based on November 2016 and February 2017, the spatial trends of the anisotropy were coherent throughout the simulation period, thus exhibiting the robustness of the methodology.

The numerical wind fields present errors below $2\mathrm{m/s}$ (**?**), which means that the V_w calculated can represent well actual wind conditions. The R_{V_w} is lower in Ebro Delta (Fig. 6 [a]) than at Tarragona (Fig. 6 [b]) due to the following reason: the orography at the Ebro delta is flat, and wind blows from a wide range of directions; whereas Tarragona features mountain chains that channel the winds into a more limited directional subset. The anisotropy pattern at Begur (Fig. 6 [d]) may be explained due to the strong Mistral and Eastern winds (**??**), that both affect nearshore and deep waters.

Hence, the behaviour of R_{V_w} near the coast can ~~, nevertheless~~ show sharp local variations due to the joint effect of orography, mesoscale circulation and large-scale circulation, all affecting wind strength and directionality. However, the seasonality does not affect R_{V_w} as much. In all cases V_w becomes more isotropic towards the offshore, denoting a decreasing control by the land-water boundary.

The R_{H_s} pattern is similar, with wave fields showing boundary effects (mainly in directional properties) for coastal distances below 50km, which has also been considered an order of magnitude estimate for land wind effects. Farther from the coast there is a clear trend to isotropy, more pronounced for transects with more stable atmospheric conditions. The link between R_{H_s} and land-originated winds can be appreciated by the shift from homogeneous to anisotropic behaviour in the northern most transect (Begur) where the effect of V_w on H_s is only evident up to $38\mathrm{km}$ from the coast. Note that in the Ebro Delta shows a more isotropic value at the coastal zone. This area presents a wider continental shelf than the other profiles, then wave dissipation and refraction tend to be more homogeneous. Henceforth, more anisotropic winds plus a steeper profile may be considered as the main reasons for the discrepancies among the beach profiles.

Such behaviour of R_{H_s} with coastal distance parallels that of particulate matter diffusivity, which tends to become isotropic at around $10\mathrm{km}$ (**?**) from the land-water boundary. The degree of geo-statistical anisotropy in diffusivity is physically related to eddy kinetic energy, which varies as $x^{5/4}$ (x being separation distance) for depths below $20\mathrm{m}$ (**?**). A steep bottom slope will favour deep-water wave behaviour at relatively short distances from the coast, as shown by the distinctive behaviour of R_{H_s} for coasts of different slope. However, although R_{H_s} presents greater variance (more outliers) for steep slopes (e.g. the due to the combination of deep and shallow water wave regimes as in the central-north transect, near Mataro harbour) the gradient of

R_{H_s} with distance to the coast is similar for all types of bathymetry considered, suggesting a generic value of the proposed approach. This is also true for any time of the year.

The coastal boundaries suggested by **?** for the Catalan Coast can be 0.1-0.6km (frictional coupling of fluids between shelf and nearshore), 10km (non-linear coupling between shelf and slope), 1km (non-linear coupling between shelf and nearshore), among other suggested values of the same order of magnitude. The l provided in our analysis is slightly larger than the value given for the frictional coupling of fluids between shelf and nearshore, whereas it is similar or smaller than in the non-linear couplings. Nevertheless, the orders of magnitude are similar.

The ρ parameter of the Gaussian copula, characterizing the dependence structure among R_{V_w} and R_{H_s} reflects a certain similarity of the spatial behaviour for both variables, R_{V_w} and R_{H_s} (see Figs. 6 and 7). The overall mutual dependence of R_{V_w} and R_{H_s} is strongest for the northern-most transect (Begur), where the topo-bathymetric control of the Pyrenees and their submerged signature becomes better defined. Such mutual dependence gets weaker for the central and southern coastal transects (see Fig. 10). There seems to be a strong wind channelling aligned with the main river valleys ~~(?)~~ (??) in February and March, dominating the local wave fields. The ρ parameter should reflect this spatial and temporal variation, resulting in a coastal zone width that will be a function of the prevailing met-ocean drivers and should thus be considered as a dynamic concept.

The resulting coastal definition ~~will~~ can be data (numerical or observed) driven, being directly applicable to any region with a forecasting system or with enough coverage of in-situ plus satellite data. The proposed criteria appear to work well for wave-dominated and micro-tidal environments, and although suitable for any combination of factors, their application to macro-tidal regimes or river-discharge dominated areas should account for the corresponding signature in the hydrodynamic fields. Under these conditions the preferred variable could change to current velocity or to temperature, considering in all cases the effect of spatial resolution in the results.

7 Conclusions

The proposed coastal fringe (water sub-domain) definition is based on an objective estimation of the geo-statistical anisotropy as a proxy for the influence of the land border. The suggested statistical assessment can be applied to any variable that reflects such an influence (here it has been illustrated with wind velocity and significant wave height) and can be easily automated for any field, numerical or observational, that presents enough resolution.

The methodology has been tested with numerically generated fields, ~~supported by~~ validated with datasets from Puertos del Estado buoys and altimeter. Anisotropies of wind velocity and significant wave heights have been extracted along a set of characteristic profiles spanning widths up to 100km (see Fig. 2), considered sufficient for the relatively narrow shelfs in the Spanish Mediterranean coast. The performed analysis has shown how wind and wave fields are influenced by the land-sea border, demonstrating the topo-bathymetric control on met-ocean factors. This control depends on topographic (mountain chains and river valleys) and bathymetric (bottom slope, submarine canyons or prodeltas) features but also on the energetic level of the prevailing weather, leading to a dynamic definition of the coastal water domain. The resulting widths, based on variance

variation, span distances in the kilometre range, depending on bottom slope and coastal plan shape geometry. The correlation between the wind and wave based definitions (i.e. the mutual dependence among R_{V_w} and R_{H_s}) seems to be stronger in the northern-most parts of the study area, where the topo-bathymetric control is most prominent.

This new definition of the coastal zone can be useful for setting up standards to delimitate this transitional fringe, facilitating the selection of processes and boundary conditions for modelling and providing an objective coastal zone limit for impact assessments. Such an approach can also support directional and asymmetric measures of error and the underlying metrics (between model and data), leading to improved products and standards in the coastal zone.

Acknowledgements. This paper has been supported by the European project CEASELESS (H2020-730030-CEASELESS) and the Spanish national projects COBALTO (CTM2017-88036-R) and ECOSISTEMA-BC (CTM2017-84275-R). As a group, we would like to thank the Secretary of Universities and Research of the department of Economics of the Catalan Generalitat (Ref. 2014SGR1253). We duly thank the Meteorological Office of the United Kingdom for the provided wind fields~~and~~, Copernicus Marine Environment Monitoring Service for the altimeter data, and Ente Publico Puertos del Estado for the ~~wave observations~~in-situ measurements.

Reviewer #1

GENERAL COMMENTS

This study is aimed at assessing the definition (say distance from the coast) of land-sea boundary. For this purpose, wind (from UKMO) and wave (using SWAN) model data are used. No additional oceanic/atmospheric variables are taken into account. The whole analysis is based on the calculation of anisotropy of 2-D fields, which is computed along four transects of the Catalan Coast (used as test site). The paper is well-written, but it lacks a connection with other methods currently employed to define that boundary (e.g. using oceanic variables, as salinity, or depth) and uses an unique strategy (anisotropy + quantile threshold) for the identification of the boundary. In my opinion the paper can be improved and worthy to be published after a major revision that assesses the stability of the boundary computation and its seasonality.

SPECIFIC COMMENTS

Title.

Since the definition is based on wind and waves I suggest mentioning them in the title. Or at least making it clear that in the study a methodology is proposed (which can be then used with other variables).

Thank you so much for the suggestion. We have adapted our title to it. The article has been renamed as: “The land-sea coastal border: A quantitative definition by considering the wind and wave conditions in a wave-dominated, micro-tidal environment.”

Abstract.

“The more robust estimator [...]”. How the robustness of the estimators expressed? Did authors check, for example, the sensitivity of the results on the quantile threshold?

(pp. 1, line 6) We have changed “robust” by “viable”, as the selection of the 90th percentile is a convention commonly followed in Literature (Eastoe 2013, Bernadara 2013).

Can authors show the distribution function of anisotropy for wave and wind fields?

(pp. 1, line 7) It is the 90th quantile of the variance of the anisotropies. We have

rectified by introducing this specification in the text.

Introduction.

The land-sea border problem is presented by means of references mostly pointing to the same group that wrote the paper. My suggestion is to improve the overall view of the problem. o It seems to me that other references are more appropriate for the SWAN model.

The state-of-the-art has been improved with recents works in the same study area.

The number of citations from the same group has been reduced. Here is a list of the ones that have been obviated:
-Bolaños and Sánchez-Arcilla (2006), as it can be represented by Bolaños et al. (2009).
-Bolaños et al. (2007), as it only appears once in the text and along other references.
-Pallarés et al. (2013), for the same reason.
-The thesis of E. Pallarés can be represented by Pallarés et al. (2014).
-Sánchez-Arcilla et al. (2008), as it is similar to Bolaños et al. (2009).
-Sánchez-Arcilla et al. (2016), as it only appears once, and along with another reference. Also, it is more about ports.
-Sierra et al. (2017) has been obviated, as it is well represented by the other bibliography that accompany it in the “Introduction”.

It has been added references, not only about the SWAN model, but on spectral wave modelling as well:

Bertotti, L., Bidlot, J., Bunney, C., Cavaleri, L., Passeri, L. D., Gomez, M., Lefe, J., Paccagnella, T., Torrisi, L., Valentini, A., and Vocino, A.: Performance of different forecast systems in an exceptional storm in the Western Mediterranean Sea, Quarterly Journal of the Royal Meteorological Society, 138, 34–55, https://doi.org/10.1002/qj.892, https://rmets.onlinelibrary.wiley.com/doi/abs/10.1002/qj.892, 2012.

Booij, N., Ris, R., and Holthuijsen, L.: A third-generation wave model for coastal regions, Part I, Model description and validation, Journal of Geophysical Research, 104 (C4), 7649–7666, 1999.

Cavaleri, L., Bertotti, L., and Pezzutto, P.: Accuracy of altimeter data in inner and coastal seas, Ocean Science Discussions, 2018, 1–13, https://doi.org/10.5194/os-2018-81, https://www.ocean-sci-discuss.net/os-2018-81/, 2018.

Lionello, P. and Sanna, A.: Mediterranean wave climate variability and its links with NAO and Indian Monsoon, Climate Dynamics, 25, 611–623,

https://doi.org/10.1007/s00382-005-0025-4, 2005.

Qi, J., Chen, C., Beardsley, R. C., Perrie, W., Cowles, G. W., and Lai, Z.: An unstructured-grid finite-volume surface wave model (FVCOM-SWAVE): Implementation, validations and applications, Ocean Modelling, 28, 153 – 166, https://doi.org/https://doi.org/10.1016/j.ocemod.2009.01.007, http://www.sciencedirect.com/science/article/pii/S1463500309000067, the Sixth International Workshop on Unstructured Mesh Numerical Modelling of Coastal, Shelf and Ocean Flows, 2009.

Roland, A. and Ardhuin, F.: On the developments of spectral wave models: Numerics and parameterizations for the coastal ocean, Ocean Dynamics, 64, 833–846, 2014.

Roland, A., Zhang, Y. J., Wang, H. V., Meng, Y., Teng, Y.-C., Maderich, V., Brovchenko, I., Dutour-Sikiric, M., and Zanke, U.: A fully coupled 3D wave-current interaction model on unstructured grids, Journal of Geophysical Research: Oceans, 117, https://doi.org/10.1029/2012JC007952, https://agupubs.onlinelibrary.wiley.com/doi/abs/10.1029/2012JC007952, 2012.

Staneva, J., Wahle, K., Günther, H., and Stanev, E.: Coupling of wave and circulation models in coastal-ocean predicting systems: a case study for the German Bight, Ocean Science, 12, 797–806, https://doi.org/10.5194/os-12-797-2016, https://www.ocean-sci.net/12/797/2016/, 2016.

Wiese, A., Staneva, J., Schulz-Stellenfleth, J., Behrens, A., Fenoglio-Marc, L., and Bidlot, J.-R.: Synergy of wind wave model simulations and satellite observations during extreme events, Ocean Science, 14, 1503–1521, https://doi.org/10.5194/os-14-1503-2018, https://www.ocean-sci.net/14/1503/2018/, 2018.

WISE Group: Wave modelling-the state of the art, Prog. Oceanogr., 75, 603–674, 2007.

Zijlema, M.: Computation of wind-wave spectra in coastal waters with {SWAN} on unstructured grids, Coastal Engineering, 57, 267 – 277, https://doi.org/http://dx.doi.org/10.1016/j.coastaleng.2009.10.011, http://www.sciencedirect.com/science/article/pii/S0378383909001616, 2010.

Theoretical background.

I warmly suggest improving this section to make the reader more familiar with the concept of anisotropy. A couple of examples (high anisotropy, low anisotropy) using different set of wave/wind data will help to familiarize with the concepts here presented.

A clarification has been added to the introduction (pp. 2, line 15): “A wind or wave field that has a high anisotropy can present a predominant wind or wave direction, respectively.” The interpretation of the geometric anisotropy values and the possible underlying physical processes are included throughout the Discussion section.

(pp. 15, lines 5-6) The phrase: “ which facilitates multiple simulations to perform a statistically stable analysis of anisotropy” is misleading and is not very much informative. Thus, it is eliminated.

The definition of R seems not to be consistent with the one given by Chorti and Hristopulos (2008). I suggest improving the presentation of the method.
(pp. 3, lines 2-7) We have improved the definition as: “Given a spatio-temporal field X(s, t), where s stands for a 2-D vector (zonal and meridional components) and t is the time, it is assumed that the iso-level contours of the correlation functions are invariant, i.e. ellipses in two dimensions. The main axis of these ellipses are termed u and v, respectively (see Fig. 1). The metric of the geometric anisotropy, then, becomes their ratio R = u / v (R exists [0, inf)) (Chorti and Hristopulos, 2008; Petrakis and Hristopulos, 2017). An R value close to unity means that u and v are isotropic, i.e. homogeneous across the different directional sectors. As R increases, the difference between the main axis increase, showing higher anisotropy at certain directional sectors.”

Is there a difference between the adopted method and others used to compute the consistency of spatial fields, such as the structure tensor?
We understand that the structure tensor is a similar concept to the anisotropy, but what we do here is to put emphasis on the anisotropy of the wind and wave conditions near the coast and to statistically quantify its spatial distribution.

For the Copula function, I suggest changing (u, v)-variables with other symbols as they are already used for the definition of anisotropy.
We have proceeded as suggested.

Methods

How the covariance of anisotropy is computed?

The covariance matrix is computed following (Chorti and Hristopulos, 2008):

From a X(s,t), where s is a 2D-vector (zonal (i) and meridional (j) component) and t is the time. We assume, for each time step:

1. The covariance matrix Q can be computed: Q(i,j) = E [dX(s)/ds(i); dX(s)/ds(j)]

Where E[·] are the ensemble averages.

I suspect the wind model resolution is not 2.5 and 3.75 . However, were they km (instead of degrees), the model seems not to be enough resolved to provide accurate data at 2-3 km scale, which is the final value provided for the border. The SWAN model at 600 m close the shoreline is at limit in this respect (the border encompasses 3-4 grid points). Can authors comment on this aspect?

Thank you for the remark. The spatial resolution of the wind fields is 17 km. It has been corrected in the paper.

We agree that a spatial resolution of 600 m could not be enough for solving wave breaking and shallow water processes along the whole coastline. However, such a resolution can provide a good assessment on wave generation and propagation (please refer to the error metrics in Table 1 and Figure 5.

The use of unstructured meshes avoids nesting, that may be an important source of uncertainty. This work shows that the continental shelf (mainly, the inner shelf) joint with the wind fields patterns, are strongly correlated with the wave fields.

Additionally, we have previously dealt with this issue by carrying out an inverse distance weight type of interpolation in order to gain resolution, before computing the geo-statistical anisotropy of Vw and Hs.

If you define the resolution in meters, I guess it is smaller near the coast, not higher.

We have substituted “higher” by the term “denser”, in order to make the text clearer to the reader.

Which period is spanned by the analysis? (February 2017? Why not using a longer period, say 2016-2017?).

The period ranges from November 2016 to March 2017. Such limitation comes from the availability (at the moment of writing) of the wind fields.

As far as waves are concerned, using the proposed methodology, the distance of the border should change between August (instead of November, Fig. 9) and February. A season-based classification of the border would be a sound improvement of the paper.

As mentioned above, unfortunately, the authors do not have data for August.

We agree that the anisotropy of the wind and wave fields may depend on seasonality. However, according to our data, the 90th percentile of the variance of the anisotropy does not depend on the seasonality. We would like to make an emphasis that it is the quantile, and not the absolute value, that stays the same throughout the year.

About the radius and quantile threshold. Those two values seem to me quite arbitrary and not directly physically-based. Authors could do a sensitivity analysis to show how the results depend upon those values (the quintile, in particular). This is an important task in order to evaluate the stability of the proposed methodology (and then make it usable in other contexts) and provide the uncertainty of the location of the boundary. o It would be useful to plot the quantile values on the heatmaps.

The 90th percentile in an environmental parameter (e.g. Hs) is a convention commonly followed in Literature (Eastoe 2013, Bernadara 2014). We have used this same idea, applied to the variance of the geo-statistical anisotropy of Vw and Hs. This concept is illustrated on Figs. 8 and 9.

Please explain what is the count in the heatmap's caption?

The comment "The counts are the number of elements within a hexagon.
" has been added to Figs. 6 and 7.

Additionally, the following text has been added (pp. 7, lines 7-11): Heatmaps are used to represent the spatial distribution of the geo-statistical anisotropy, showing how the density of R behaves as a function of distance to the coast and time (see Figs. 6 and 7). These maps are scatter plots that act as a 2D-histogram, in which two variables (in this case, R and distance to the coast) are grouped in pre-defined intervals. The elements selected to aggregate samples for the heatmap are hexagons with side 5km and a scale for anisotropy of 20 units for both R(Vw) and R(Hs) .

I suggest putting the wave model assessment in a dedicated sub-section

separated from the results of the anisotropy analysis.
The appearance of the validation graphs along with the text for the anisotropy analysis is because of the limitations of the LaTeX file. We are certain that the figures will appear along with the text, in the final version.

Is there a reason why in the panels of Fig 8 and 9 the dashed green vertical lines are not aligned (horizontal axes seem consistent)?
The figures are about 1 mm narrower above because of the number of digits in the y-axis. We believe that it should not significantly interfere in the interpretation of the graphs.

Reviewer #2

Review: "The land-sea coastal border: A quantitative definition", by Sánchez-Arcilla et al.

Recommendation: major revision.

Summary: The authors attempt to provide a quantitative and generalizable definition of "land-sea" zone, i.e., cross-shore width of that particular marine area that is strongly affected by the presence of the continent. The methodology is based on the measure of anisotropy of specific, vectorial and/or scalar fields of environmental parameters. For this work, the authors use wind velocity and significant wave height from well-calibrated and validated numerical outputs.

General comments

The work the authors present is really intriguing and I particularly like the idea of defining a "coastal zone" by using environmental variables in a quantitative fashion. However, while the specific variables the authors consider in this application (i.e. wind velocity and significant wave height) are particularly suitable for the study area they might not work for a different environment, where, for instance, wind and wave patterns do not actually characterize the coastal zone. As stated by the authors, river plumes or, more in general, bio-geochemical processes may lead for a better definition of a "coastal area" and, as a consequence, the methodology here proposed might not be suitable. All this is at the base of my main criticism:
to state that such a methodology provides a "quantitative definition for the land-sea (coastal) transitional area" is too strong; although I like generalizations, I still believe that a "land-sea (coastal) transitional area" can be defined by starting from the specific physical, and/or biogeochemical, and/or geological, and/or ecological process we want to investigate.
(pp. 5, lines 8-12) The following definition has been added to the text: "Although other definitions of the coastal boundary can be based on river plumes or bio-geochemical processes, it has been intended to focus on a more hydro-dynamical expression of such boundary for wave-driven coasts."
We have also specified through the text (Abstract, Introduction and pp.5) that we only focus on wave-driven environments.

A second comment regards the poor connection between the pure mathematical/statistical part and the environmental application. I would have

appreciated a better explanation of the statistics by starting from the environmental data, also discussing physical meanings and assumptions. To present the theoretical background as it is leaves the reader with some doubts regarding the feasibility of the methodology.
(pp.5, lines 5-8) It is intended to show that, as one approaches the coast, the wind and the wave fields should present a higher geometric anisotropy, that is, they should present predominant wind and wave directions. Furthermore, there should be a geo-statistical boundary to the value of this anisotropy that could help define a coastal boundary.

<u>Specific, minor comments</u>

Abstract - replace "perpendicular" with "cross-shore" in line 2
The suggested change has been carried out.

Introduction - The are several definition of what a Land-sea border is (Shaw et al., 2008; Geleynse et al., 2012). I would avoid (at least, at the beginning) to frame the land-sea border within this specific definition. Instead, it would be better to state that over land-sea border areas occur specific met-ocean dynamics that actually characterize land-sea coastal border. The aim of this work is to quantitative define the extension of this area. (see general comment).

We agree with this. Hence, the definition by Wright is obviated from the "Introduction".

Thank you very much for the references. The text has been revised as follows:

"There is, thus, a need for a systematic and objective definition of the coastal fringe that considers underlying processes and that has general applicability allowing for the time/space dynamics of this fringe. This type of approach has been explored in the literature, where for instance Sánchez-Arcilla and Simpson (2002) reviewed a number of possibilities based on a dynamic balance of competing processes (i.e. drivers) such as inertial effects, geostrophic steering, sea bed friction or water column stratification. Another suitable option is to focus on the consequences of such processes, such as the nearshore morphodynamic features (Geleynse et al., 2012) (i.e. deltas, sand spits, overwash fans, beach berms). Both complementary classifications requires spatial data that needs to be updated accordingly within timescales that may range from years (i.e. long-term erosion due to sea level rise) to days (i.e. storm-scale)."

- "Sentinel data" (in line 3-pag 2) ; the general reader might not be familiar with

the sentinel missions and, therefore, might not understand that here authors are referring to satellite data. Please, introduce the Remote Sensing approach properly.

This version does not put so much emphasis on the Sentinel satellites, but rather on wave altimeter data in general. The following sentences replace the original lines 3 and 4: “The recent advent of high resolution and short revisit time provided by them offer an alternative source of information for such a coastal zone definition although with some limitations since the data may start degrading at a few kilometres (order 10km) offshore from the coast (Cavaleri and Sclavo, 2006; Wiese et al., 2018; Cavaleri et al., 2018).”

- “Because of that” (in line 5-pag 2); Please, be more specific. It’s not clear the use of Sentinel data in defining land-sea limits and what the authors mean with degradation of data. “necessary”; too strong, I would write “useful” rather than necessary.

The following sentences replace the original lines 5 to 8: “ The land boundaries induce error in the satellite observations. Hence, it is useful to use high resolution numerical simulations supported by in-situ data so that land-sea boundary effects are properly captured for the subsequent coastal definition that will be based on the inhomogeneity introduced by the presence of the land boundary.”

- “coastal anisotropy” (in line 13-pag 13); I would write “anisotropy of environmental parameters” rather than coastal anisotropy

The suggested change has been carried out. The following sentences replace the original lines : “The aim of this paper is to analyse the geo-statistical anisotropy of nearshore wind and waves, in wave-driven coasts. From that, what follows is to propose a new quantitative and objective definition for the land-sea border that benefits from these high-resolution (spatial and temporal) fields and from the underlying process-based knowledge. This definition can be useful to determine a set of criteria for numerical purposes (e.g. nesting coastal domains) but also for more practically oriented applications (e.g. offshore limit for outfall dispersion).”

Theoretical background - G(x) in line 10 should be G(y), as far as I am missing something;

The recommended correction has been carried out.

As I suggest in the General Comments, this section would be much clearer (and the ms much stronger) if the theoretical background is explained by starting from environmental variables. As it is, the reader might get confused.

Thank you so much for the recommendation. We would like to leave the explanation with environmental variables to the Methodology. The Theoretical background is intended to be an introduction of the mathematical tools used.

Study area - By reading the section it comes natural to think that the analysis is particularly suitable for this study area, thus difficult to generalize

It is intended to propose this methodology. The proposed limit to the coastal fringe is not to be generalized, but the methodology can help find the indicated one for each coast.

References

Shaw, J. B., Wolinsky, M. A., Paola, C., & Voller, V. R. (2008). An image based method for shoreline mapping on complex coasts. Geophysical Research Letters, 35(12).

Geleynse, N., Voller, V. R., Paola, C., & Ganti, V. (2012). Characterization of river delta shorelines. Geophysical Research Letters, 39(17).

Reviewer #3

GENERAL COMMENTS:
The paper addresses a relevant scientific question which is well within the scope of Ocean Science. The authors present a methodology with the aim to quantitatively define the land-sea boundary in wave-dominated and micro-tidal environments. The presented methodology builds on met-ocean datasets which are well-known and frequently used in the field. The authors conclude that the proposed land-sea boundary (coastal fringe) definition is a generic method. However, as also stated by the author, the correct choice of met-ocean or biogeochemical variables might be case dependent and the presented application is tailored to the case specific conditions at the Catalan coast.

It would significantly improve the general applicability of the method if the authors could briefly describe how one should choose the variables that reflect the influence of the land border in a specific application.
(pp. 5, lines 5-8) The following definition has been added to the text: “Although other definitions of the coastal boundary can be based on river plumes or bio-geochemical processes, it has been intended to focus on a more hydro-dynamical expression of such boundary for wave-driven coasts.”

Moreover, by comparing the results to other land-sea border definitions (validation) and by providing uncertainty estimate of the computed coastal zone limit the authors would make the methodology stronger.

Thank you very much for the remark. We have added several comments on this issue throughout the paper. Please find two examples below:

(pp. 2, lines 1-8) *“There is, thus, a need for a systematic and objective definition of the coastal fringe that considers underlying processes and that has general applicability allowing for the time/space dynamics of this fringe. This type of approach has been explored in the literature, where for instance Sánchez-Arcilla and Simpson (2002) reviewed a number of possibilities based on a dynamic balance of competing processes (i.e. drivers) such as inertial effects, geostrophic steering, sea bed friction or water column stratification. Another suitable option is to focus on the consequences of such processes, such as the nearshore morphodynamic features (Geleynse et al., 2012) (i.e. deltas, sand spits, overwash fans, beach berms). Both complementary classifications requires spatial data that needs to be updated accordingly within timescales that may range from years (i.e. long-term erosion due to sea level rise) to days (i.e. storm-scale).”*

(pp. 16, lines 13-17) We have added the comment: *"The coastal boundaries suggested by Sánchez-Arcilla and Simpson (2002) for the Catalan Coast can be 0.1-0.6km (frictional coupling of fluids between shelf and nearshore), 10km (non-linear coupling between shelf and slope), 1km (non-linear coupling between shelf and nearshore), among other suggested values of the same order of magnitude. The "l" provided in this analysis is slightly larger than the value given for the frictional coupling of fluids between shelf and nearshore, whereas it is similar or smaller than in the non-linear couplings. Nevertheless, the orders of magnitude are similar."*

The scientific methods and assumptions are in general valid and clearly outlined, even though further clarifications are required at certain sections (see specific comments). The paper is well structured in general; however, certain elements should be better explained (see specific comments).

SPECIFIC COMMENTS:

Title:

- The title should indicate that the methodology to quantitatively define the land-sea coastal border was only tested for a case study in a wave-dominated and micro-tidal environment.

The new title is adapted to this idea: "The land-sea coastal border: A quantitative definition by considering the wind and wave conditions in a wave-dominated, micro-tidal environment".

Abstract:

- I propose to change the term "90th quantile" to "90th percentile" throughout the paper. The authors refer to the 90th 100-quantile which is called percentile.

Thank you very much for this remark. Therefore, we have substituted "quantile" by "percentile".

Study area:

- The authors state (page 4, line 5) that the focus area is the Spanish north-eastern Mediterranean coast due to the availability of in-situ and Sentinel images for support. It is not clear how the Sentinel images were utilised in the methodology as a support (unless they were used for the SWAN model validation, which is not stated in the paper).

We agree with this point. Please refer to the answer below, to the same referee, referring to Fig. 5.

Methods:

- Further background information on the Unified Model and/or the wind field data should be given. The wave data is explained in much more detail

compared to the wind data.
(pp. 6 lines 4-10) The following explanation has been added to the text: “There are two atmospheric prognostics: the dry one (three-dimensional wind components, potential temperature, Exner pressure and density) and the moist one (specific humidity and prognostic cloud fields (Walters et al. (2011)). Both long and short radiations (from the sun and the Earth itself) are included, whereas the effect of aerosols reflecting them is taken into consideration.”

- According to Cullen (1993) the operational forecast grid for the Unified Model is 0,833 degree (latitude) and 1,25 degree (longitude), whereas the standard climate and upper atmosphere configuration uses 2,5 degree (latitude) and 3,75 degree (longitude). Is it really the second configuration which is used in this paper? This resolution would mean approximately 250km (latitude) and 310 km (longitude). That is a very coarse resolution for this purpose.

Thank you very much for this remark. The horizontal resolution of the atmospheric model was a gridsize of 17 km, the same that the UK Met Office global deterministic forecast model. (pp. 6, 12-13) “The computational domain of the wind field spans the whole Mediterranean Sea using a regular grid with spacing of 17km and a time step of 1h.”

Also, we have improved the flow chart to clarify, along with the existing definition of the methodology, that we interpolate the wind/wave data field in order to obtain a finer grid from which to compute the geo-statistical anisotropy along the transects.

- I suggest adding steps to the methodology figure (Figure 3) for the wave and wind model validation, interpolation, as well as for the distribution fitting (Gaussian copula model).

We have proceeded as indicated. The caption of the figure is also modified: “Flow-chart summarizing the methodology used in this paper. The dashed blue rectangle represents the input data, the red dashed rectangle indicates the output data. Only the wind velocity is obtained from an external source, the rest of the steps have been carried out for this analysis. Rectangles indicate data generation (input/output) and rhombuses the subsequent analyses of the proposed methodology.”

- It is mentioned (page 6, line 9) that wave fields have been validated. Validation results should also be included for the wind field data. Reference to the wind field validation is only given in the discussion section (page 15, line 3-4). I suggest moving this sentence to the Methods section where the United Model is described.

Validation of the wind fields is not included in this paper. Then, we have added the following: (pp. 5 line 26) “These wind data are validated in (Martin et al. ((2006)).”

- Is there any reason why the 90th percentile is used in equation 6? Is it based on expert knowledge or literature?
Indeed, the selection of the 90th quantile is a convention commonly followed in Literature (Eastoe 2013, Bernadara 2014).

Results:
- The figures 6,7,8,9 are presented on pages 11-to 14 while described on page 7. This makes it hard for the reader to follow the paper. Consider to move them closer to the place where they are described.
We agree with this suggestion. The figures appear after the text, in the source file. This problem happens because the graphs are large and self locate in these pages. We believe that this phenomenon would only occur in this pdf format, but it should be automatically solved in an online edition.

- In Figure 5 red dots are labelled as Altimeter data. Is this data coming from Sentinel images? If yes, please explain both in the legend and in the text, and also add which mission it is (e.g. 3A).

The altimeter data comes from Jason-2, Jason-3 and Cryosat. Sentinel 3A data has not been used in this contribution.

(Fig. 5) We have added the clarification: "The red dots are altimeter data from altimeter data (Jason 2, Jason 3 and Cryosat)"
(pp. 7 line 18) We have added: "The SWAN model simulations have been validated with significant wave height (H_s), registered with buoys and altimeter data, at the southern (Tarragona location) and northern (Begur location) coastal sectors (Figs. 4 and 5)."

- The calculated coastal zone limit values are not mentioned explicitly in the results section, even though they are depicted in Figure 8-9 and mentioned in the abstract. I suggest mentioning them in the text as this is the main objective of the methodology.
We have modified the text so now it reads: "The coastal zone limit "l", corresponding to the 90th percentile of the total variance (fringe between 0
and 100km), is calculated from equation 6 (Figs. 8 and 9) and is 3km. It is consistent with time interval (month of study) and location (sector)"

- Please use the word "coastal zone limit" consistently. Sometimes it is only called "limit".
The suggested action has been carried out throughout the text (pp.10 line 1, pp. 17, line 5).

Discussion:

- The authors write that "The calculated anisotropies should be as robust as the starting wave or wind fields that are employed in the analysis" – that is why the robustness of the wind field should be better defined in the Methods section.

We agree with the reviewer. The UK Met Office wind fields has shown systematically good accuracy (see Martin et al. 2006, Brown et al. 2012, Walters et al. 2011). We have assumed that the wind fields have state-in-the-art accuracy and we have focused on validating the wave fields in the Results and we hope that this could be a valid procedure.

- Figure 6-7: the description of the hexagons in the heatmap should be added to the figure as they are only described in the text. Also, the description of the blue dashed line at 20 km should be added as in Figure 8 and 9.

The suggested changes have been performed.

- Figure 10: The x axis represents the months within a year cycle. Which year is it? And why only months 1, 2, 3, 11,12 were selected?

These months (year 2016; 11, 12 and year 2017; 1,2,3) span the available data. As mentioned above, the available wind fields ranged this timeline (at the moment of writing this paper). We accept this shortcoming as a limitation of our contribution.

The following text has been added to the caption of the figure: "The plot shows the variation with time (horizontal axis) between November of 2016 and March of 2017. The parameters are placed in a manner that they start from January."

- The authors write (page 16, line 5) that the correlation between R_Vw and R_Hs is the strongest for the Begur transect. On the other hand, in Figure 10 the Begur transect (orange dots) has a correlation parameter around 0 (max ~ 0.026). This figure indicates that the Mataro transect has the strongest correlation parameter, not Begur.

I suggest clarifying this.

Thank you for pointing this out. We have clarified in the text that it is the "overall" dependence that is stronger in Begur: "The overall mutual dependence of R_vw and R_Hs is strongest for the northern-most transect (Begur), where the topo-bathymetric control of the Pyrenees and their submerged signature becomes better defined."

References:

- The number of references is rather high (57). Moreover the share of references originating from the same authors is also high.

Although all references are of strong interest, we have followed the suggestion of the referee to reduce the number of references. Here is a list:

-Bolaños and Sánchez-Arcilla (2006), as it can be represented by Bolaños et al. (2009).

-Bolaños et al. (2007), as it only appears once in the text and along other references.
-Pallarés et al. (2013), for the same reason.
-The thesis of E. Pallarés can be represented by Pallarés et al. (2014).
-Sánchez-Arcilla et al. (2008), as it is similar to Bolaños et al. (2009).
-Sánchez-Arcilla et al. (2016), as it only appears once, and along with another reference. Also, it is more about ports.
-Sierra et al. (2017) has been obviated, as it is well represented by the other bibliography that accompany it in the “Introduction”.

Additionally, it has been added new references, that the authors consider that suit better the general messages of this contribution. Note that some of these references come from the other reviewers’ suggestions.

REFERENCES

Bernadara, P., Mazas, F., Kergadallan, X. and Hamm, L. (2014). A two-step framework for over-threshold modelling of environmental extremes. Natural Hazards and Earth System Sciences, 635--647.

Brown, A., Milton, S., Cullen, M., Golding, B., Mitchell, J., and Shelly, A.: Unified modeling and prediction of weather and climate: A
25-year journey, Bulletin of the American Meteorological Society, 93, 1865–1877, 2012.

Eastoe, E. , Kouloulas, S. and Jonathan, P. (2013). Statistical measures of extremal dependence illustrated using measured sea surface elevations from a neighbourhood of coastal locations. Ocean Engineering, 68--77.

Martin, G. M., Ringer, M. A., Pope, V. D., Jones, A., Dearden, C., and Hinton, T. J.: The physical properties of the atmosphere in the new
Hadley Centre Global Environmental Model (HadGEM1). Part I: Model description and global climatology, Journal of Climate, 19,
1274–1301, 2006.

Walters, D. N., Best, M. J., Bushell, A. C., Copsey, D., Edwards, J. M., Falloon, P. D., Harris, C. M., Lock, A. P., Manners, J. C., Morcrette,
C. J., et al.: The Met Office Unified Model global atmosphere 3.0/3.1 and JULES global land 3.0/3.1 configurations, Geoscientific Model
Development, 4, 919–941, 2011.

Comment

The authors present a methodology for determining the land-sea transitional area based on the empirical distribution of anisotropy in meteorological and ocean processes. This is an interesting article, however it will be beneficial for the audience if the authors could provide some feedback on the following matters:

1 Definition of anisotropy
In [Chorti et.al., 2008] a non-parametric estimator of statistical anisotropy was proposed, for which an approximate estimate of the anisotropy statistics distribution was provided in [Petrakis et.al., 2017]. While the authors cite [Chorti et.al., 2008], from the rest of the references it is not clear if anisotropy is defined as in geostatistics (statistical anisotropy: directional dependence of correlation functions) or as in (geo)physics (directional variation of a physical property, e.g., elasticity, permittivity). Also it is not clear how anisotropy is estimated. The authors should clarify, by providing the definition of anisotropy and the estimator they use.
It is very true that we should specify that it is a geo-statistic anisotropy (geometric). Therefore, we have specified at the aim of the paper: “The aim of this paper is to analyse the geo-statistical anisotropy of nearshore wind and waves, in wave-driven coasts. From that, what follows is to propose a new quantitative and objective definition for the land-sea border that benefits from these high-resolution (spatial and temporal) fields and from the underlying process-based knowledge.”

2. Spatial resolution of wind and wave fields

For both fields there are sub-domains with anisotropy ratio estimates of R≈100 or more. Therefore, the largest correlation length within such sub-domains is larger by two orders of magnitude compared to the smallest correlation length over the perpendicular principal axis. Assuming stationarity, for an accurate estimation of anisotropy a field should be sampled at a sufficiently large domain, to satisfy ergodicity, and at a high resolution, in order to capture the spatial variability at length scales below the smallest correlation length. The authors estimate anisotropy over circular sub-domains of 5km radius. Some representative field maps would be useful to justify that the sub-domains are sufficiently large and contain an adequate number of measurement samples for the fulfillment of the aforementioned requirements.

We have modified the flow-chart to clarify that we have interpolated the wind and the wave fields in order to have enough resolution to obtain the anisotropy.

(pp. 7, lines 1-2) Also, we have reorganized the text so these lines say: “The geo-statistical Anisotropy needs to be computed on a regular grid and therefore, both wind velocity (V_w) and significant wave height (H_s) have been interpolated on a rectangular mesh, first on a grid of 1 km then to a finer mesh of 10m.”

References

Chorti, A., Hristopulos, D. T. (2008). Nonparametric identification of anisotropic (elliptic) correlations in spatially distributed data sets. IEEE Transactions on Signal Processing, 56(10 I), 4738-4751. doi:10.1109/TSP.2008.924144

Petrakis, M.P., Hristopulos, D. T. (2017). Non-parametric approximations for anisotropy estimation in two-dimensional differentiable gaussian random fields. Stochastic Environmental Research and Risk Assessment, 31(7), 1853-1870. doi:10.1007/s00477-016-1361-0